Water Science & Technology

IWA PUBLISHING

Water Science & Technology Vol 84 No 3, 524 doi: 10.2166/wst.2021.254

Kinetics, degradation mechanisms and antibiotic activity reduction of chloramphenicol in aqueous solution by UV/H_2O_2 process

Ardhendu Sekhar Giri [a,*], Animes Kumar Golder [b] and Sankar Chakma [a]

[a] Department of Chemical Engineering, Indian Institute of Science Education and Research Bhopal, Bhopal 462066, India
[b] Department of Chemical Engineering, Indian Institute of Technology Guwahati, Assam 781039, India
*Corresponding author. E-mail: agiri@iiserb.ac.in

ASG, 0000-0002-4390-8057; AKG, 0000-0001-8144-5316; SC, 0000-0002-8227-0455

ABSTRACT

In this study, the aim was to explore the effectiveness of the UV/H_2O_2 photolysis (UVP) process in terms of antimicrobial activity reduction and increasing the mean oxidation number of carbon (MONC) under the degradation of chloramphenicol (CHPL) drug. CHPL degradation kinetics and the effects of foreign anions on CHPL degradation were explored in this study. The order of the inhibition effect was found as $Cl^- > NO_3^- > HCO_3^-$ due to their different in $HO^\bullet$ radical scavenging capacity. A pseudo-first-order model for CHPL degradation was well established, and the rate constant (k_{obs}) was 2.93×10^{-2} min^{-1} ($R^2 = 0.98$) in UVP. Thirteen intermediate products were detected in MS-chromatogram and were identified through different proposed degradation pathways. The cleavage of the amide side chain in CHPL was more effective in CHPL degradation due to an electrophilic attacks by $HO^\cdot$ radicals on it. The inactivation rates of *E. coli* were decreased due to the reduction of -NO_2 group into -NH_2 functional group in CHPL that leads to the production of low toxic compounds on CHPL degradation.

Key words: electrophilic effect, hydroxyl radical, mean oxidation number, photocatalysis, toxicity

HIGHLIGHTS

- Degradation of chloramphenicol drug occurred by UV-irradiation and hydrogen peroxide together.
- $HO^\bullet$ radical formed in the presence of H_2O_2 could effectively contribute to the degradation of CHPL.
- MONC was increased with increasing the formation of daughter fragments.
- Reduction of CHPL decreases the antimicrobial activity.
- Dynamics of drug cleavage follows pseudo-first-order kinetics.

GRAPHICAL ABSTRACT

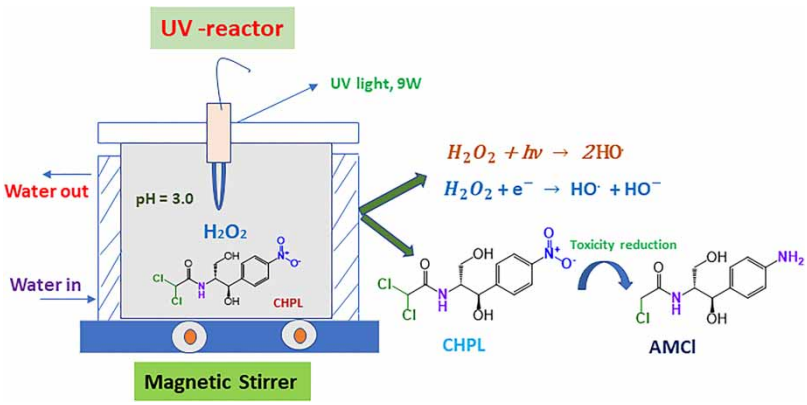

INTRODUCTION

Due to lack of proper supervision with high drug administration, the fate and occurrence of bacteria which is resistant towards many antibiotic drugs have been augmented (Brooks *et al.* 1992). The contamination occurred due to presence of varieties of antibiotic drugs in the range from ng/L to μg/L is measured as a potential threat to the environment (Liang *et al.* 2013). Chloramphenicol (CHPL) shows its activity in both gram-positive and gram-negative bacteria and is a suspected carcinogen as a broad-spectrum antibiotic (Liang *et al.* 2013). It shows its action in protein synthesis by the inhibition of microorganisms. CHPL was found to be between 0.001 and 0.031 mg/L in surface water at different places in Singapore and Korea. In effluents of sewage treatment plants (STP), it was detected between 2.08 and 26.6 mg/L in China (Trovo *et al.* 2013). Conventionally, CHPL is biosynthesized by the soil organism, *Streptomyces venezuelae* and several other *Actinomycetes* as well (Aouiche *et al.* 2012). Conventional wastewater treatment consists of a combination of physical, chemical, and biological processes and operations to remove solids, organic matter and, sometimes, nutrients from wastewater (Trovo *et al.* 2013). Preliminary treatment is used to remove coarse solids and other large materials often found in raw wastewater and secondary treatment basically eliminates the residual organics and suspended solids. Apart from these different advanced treatment processes like many homogeneous advanced oxidation processes (AOPs) UV, UV/H_2O_2, ozone (O_3), Fenton, Photo-Fenton and heterogeneous AOPs like UV/TiO_2, electro photo-Fenton, UV or solar light assisted bimetal doped catalytic processes have been used to treat the wastewater. Many essential parameters like pH of the drug solution and particulate matter have been described using different specific environmental standards like European Environment Agency (EEA) and National Ambient Air Quality Standards (NAAQS).

The detection of different generic drugs found in the aquatic environment was monitored and confirmed by studying the presence of low levels of CHPL in plants and soil (<1 μg/kg) (Hu *et al.* 2010). CHPL in Asian countries including China was noticed within the range of 26–2,430 ng/L in influent and 3–1,050 ng/L in STP effluent (Lin *et al.* 2008). CHPL concentration of 47.4 μg/L in sewage was found as it is a high consumption drug in Guiyang, China (Liu *et al.* 2009). As expected that CHPL resistant pathogens were found in different water flows (MPEDA 2010). In India, the use of CHPL has been banned in food-generating animals in 2002 (Parsley *et al.* 2010). Different conventional water treatment techniques like sedimentations, coagulation and filtration, and disinfection are ineffective in eliminating antibiotics dissolved in water (Zhang & Li 2011). The removal efficiency from the aquatic environment is extremely low due to the refractory nature of antibiotics (Boxall *et al.* 2003). Therefore, some potential treatments are necessary to degrade these antibiotics and minimize their exposure to the environment.

Studies on CHPL have been investigated in the presence of different photocatalytic processes like the Fenton process, metallic nanoparticles, microwave irradiation, and the biochemical system (Liang *et al.* 2013). Due to their economic efficacy and applicability towards real situations, these above said technologies have not yet been thoroughly evaluated despite having advantages over classical methods. Violet (UV) radiation is a promising water treatment technology and has been used to activate oxidants such as peroxides, chlorine, ozone, and ferrate to produce highly reactive radicals such as $HO^{\bullet}$ radicals (Deng *et al.* 2019).

Thus we use the UVP process which is the combination of H_2O_2 and UV radiation that has shown a great promising synergistic effect for the removal of CHPL drug as well as the inactivation of pathogens present in water. UV/H_2O_2 process that generates two $HO^{\cdot}$ free radicals by photolytic cleavage of H_2O_2, has been widely reported to rapidly and unselectively oxidize many micropollutants in water and wastewater (Deng *et al.* 2019; Wu *et al.* 2019). However, the conversion efficiency of H_2O_2 is less than 10% due to lower molar absorption coefficient of H_2O_2 at 254 nm ($\varepsilon = 18.6\ M^{-1}\ cm^{-1}$) (Miklos *et al.* 2018). Besides, most of the residual H_2O_2 requires to be quenched in a subsequent step, which increases the treatment cost (Xiang *et al.* 2016). UVP is a potential advanced oxidation processes (AOPs) that include injection of H_2O_2 in presence of UV irradiation system of wavelength 280 nm with a continuous mixing batch reactor. The O-O bond of H_2O_2 is broken in presence of UV light forming $HO^{\bullet}$ radicals (Nascimento *et al.* 2020). The reactions describing UV-photolysis are presented below (Equations (1)–(6)) (Boxall *et al.* 2003).

$$H_2O_2 + h\nu \rightarrow 2HO^{\bullet} \quad (1)$$

$$H_2O_2 + HO^{\bullet} \rightarrow HO_2^{\bullet} + H_2O \quad (2)$$

The first reaction is rate-limiting because the rate of this is slower compared to second one. In UVP, a higher initial H_2O_2 concentration produces higher $HO^{\bullet}$ radical concentration (Equation (1)), which decomposes the target compounds. However, an optimal H_2O_2 concentration exists because the overdosing of H_2O_2 leads to a reaction with $HO^{\bullet}$ radicals leaving off $HO_2^{\bullet}$ (Equation (2)). UVP is quite efficient in mineralizing PhACs (De Boxall *et al.* 2003). UV photolysis showed first-order deterioration kinetics for the decomposition of chloramphenicol drug with rate constant $6.3 \times 10^{-2}\,\text{min}^{-1}$ (Sa Da Rocha 2013).

The main aim of this study is to find out the efficacy of the UVP process to degrade CHPL in an aqueous solution and to explore the reduction of antimicrobial activity which is supported by the proposed CHPL degradation mechanistic pathways. The hydroxyl radicals ($HO^{\bullet}$) are the main species responsible for CHPL oxidation.

In order to yield the feasibility of this method for removing CHPL from its synthetic solution, we have also investigated the effect of process parameters (pH, H_2O_2 concentration, reaction time, and UV-irradiation) on degradation kinetics and the influence of foreign ions. To evaluate the toxicity reduction achieved by this process, we determined the antibacterial activity test of the UVP-treated CHPL solutions against *E. coli* pathogenic bacteria that are highly sensitive towards CHPL. Finally, intermediates obtained under the UVP process were identified, and a proposed mechanism that gave an evidence for reducing the toxicity of both unclevaged CHPL molecule and its daughter products.

EXPERIMENTAL METHODS AND MATERIALS

Chemicals and materials

CHPL drug with purity >99% (w/w) was procured from Sigma Aldrich (China). Figure 1 shows the chemical structure of CHPH. Acetonitrile (99% v/v purity) and oxalic acid (98% w/w purity) with HPLC grade were purchased from Merck (India). Sulfuric acid (98% v/v purity), NaOH (purity >98% w/w), H_2O_2 (50% v/v purity) and ethanol (purity >98 v/v %) were taken from Merck (India). For the toxicity test, *Escherichia coli* (*E. coli*) XL 10GOLD (purity >98.5% w/w) was collected from the Department of Biotechnology, Indian Institute of Technology Guwahati. Tryptone (98% v/v purity) and yeast (99% w/v purity) both were from Himedia (India). All reagents and solutions were prepared using mili-Q water (model: Elix 3, M/s Millipore, USA).

Analytical technique

A spectrophotometer (model: UV-2300) was used to analyze UV-vis spectras of CHPL and find out an optimal wavelength with the maximum absorption with an optical path length of 1 cm procured from Thermo Scientific (India). CHPL concentration was determined using high-performance liquid chromatography (HPLC). C_{18} column as a stationary phase with 25 mm in length and 4.6 ID mm was employed. A UV-Vis detector was placed in the HPLC instrument (model: LC-20AD) of Shimadzu (Japan). A mixture of acetonitrile and oxalic acid (0.01 M) (40:60 v/v) was used as the mobile phase at a flow rate of 0.5 mL/min. CHPL daughter ions identification was carried out using liquid–chromatography-time-of-flight mass spectrometry (LC-TOF-MS) system (Aquity UPLC and Waters Q-Tof Premier). Total organic carbon (TOC) measurements were made with a TOC analyzer (model: 1030C Aurora) of O.I. It was operating at 680 °C furnace temperature. Measurement of TOC by the non-dispersive infrared method, and the analyzer was equipped with an IR detector with an autosampler. pH meter (model: pH/ion 510) was used to measure pH of the solution obtained from Eutech Instruments (Malaysia).

The number of colonies forming unit (CFU) of *E. coli* bacteria was recorded to measure the toxicity of CHPL and its degradation products. Luria–Bertani (LB) media (yeast extract 5, tryptone ten and NaCl 10 are in g/L) was used for this antimicrobial test. The reaction mixture was autoclaved (model: 7407PAD, Medica Instrument Mfg. Co., India) for 30 min

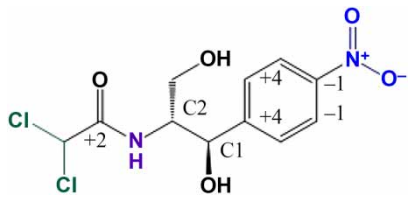

Figure 1 | Chemical structure of Chloramphenicol drug with MONC.

under 39.7 psi (abs) pressure (120 °C) after adjusting the pH at 7.0 using 0.5N NaOH. A mixture of 50 μL initial cultured of *E. coli* and 5 mL media was incubated for 24 h at 30 °C on an orbital shaker at 250 rpm (model: ORBITEK^{R}, Scigenics Biotech, India). The residual H_2O_2 present in the CHPL solution was removed after the UVP process using catalase enzyme before performing the toxicity assay (Shen *et al.* 2016). The cultured cells now made a growth media and explored into three sections. About 1–2 mL diluted growth media was added on the agar plate (APHA 1998) and the number of CFU was counted at 30 °C after 24 h of incubation. The absorption intensity of the second sample was recorded at 621 nm after diluting at different proportions. A calibration curve was then prepared by plotting the number of CFU/mL versus the absorption intensity.

The supernatant obtained from the third sample was rejected after centrifugation at 2,000 rpm for 20 min, and the collected bacterial cells were swept away using deionized water. LB media (100 mL) was used for the suspension of these collected bacterial cells and further diluted to have CFU/mL of $\sim 2.4 \times 10^8$. About 5 mL of the CHPL sample and 1 mL of cultured media withdrawn at different time interval was mixed and incubated for 24 h at 35 °C (Giri *et al.* 2014). The calibration curve was then used to find out the equivalent absorbance after transforming in terms of CFU/mL unit.

Photocatalytic experiment

Experiments were performed to investigate the CHPL degradation study under the UVP process maintained at 25 °C. The initial concentration of CHPL with 100 mg/L (TOC, 31.3 mg/L) was taken in this UVP as CHPL has a larger ability to form chelate complexes with different metals at higher concentration (Luis *et al.* 2009). Usually, in municipal wastewater treatment plants, high concentration of CHPL is not found. The antimicrobial activity, degradation kinetics and its biodegradability index were evaluated with CHPL concentration of 214 mg/L (Zuorro *et al.* 2014).

A batch experiment with the continuous stirring was explored for the CHPL degradation study. A cylindrical vessel made of borosilicate (Ø 10.5 cm) with a capacity of 1,000 mL was used as the reactor. Solution pH was adjusted by 0.05 N H_2SO_4 prior to addition of H_2O_2 and mixed at 300 rpm for about 10 min on a magnetic stirrer (model: Spinot 6,020; stirring bar: length 40 mm, Ø 0.8 mm) made by Tarson (India), and then pH of the reaction solution was further noted. The predetermined amount of H_2O_2 was added in the calculated amount of CHPL solution to achieve the final volume of 400 mL. After 1 min with the progression of the photoreaction, 10 mL sample was withdrawn, and 1 mL of 0.1 (N) NaOH was immediately added to stop the reaction by quenching of $HO^{\cdot}$ radicals. The pH was increased with the addition of NaOH to 12.5. Photolysis of H_2O_2 producing $HO^{\cdot}$ radical (Equation (1)) is tremendously fast at such high pH (Levard *et al.* 2013; Giri & Golder 2014).

The temperature of clear supernatant was increased to 60 °C to eject residual H_2O_2, if any. 80 μL and 5 mL clear solution was taken out to determine CHPL and TOC concentrations, respectively. 0.45 μm cellulose filter was used to filter the remaining liquid. About a 2 mL sample was used to determine the mass spectra. Likewise, under UV light alone, a blank experiment was also performed without addition of H_2O_2. An UV lamp (intensity: ~ 9 W and wavelength: 362 nm) obtained from Hong Kong Jie Meng International Lighting Ltd Company (China) was hired for this work. Based on our earlier studies, the UV light intensity was selected in this study (Giri & Golder 2014). The UV-lamp was fixed at 5 cm above from the top of drug solution. The temperature of the reaction mixture was properly controlled using a cooling arrangement (25 ± 2 °C).

RESULTS AND DISCUSSION

Dynamics for CHPL and TOC removal at optimal condition

UVP treatment was significantly faster than UV process alone upon CHPL degradation (Figure 2). For the maximum amount of CHPL removal, pH, H_2O_2 concentrations and UV-intensity varied from 1.5 to 4, 5 to 20 mM, and 5 to 12 W, respectively (Figs S1 to S3). The preliminary experimental trials were done in the presence of a selected value of UV-intensity with changing pH values from 1.5 to 4 and concentration of H_2O_2 prior to the experiment. After that, UV-intensity and H_2O_2 doses were adjusted at the fixed pH value obtained in the provisional run. Again, pH was changed from 1.5 to 4 with the finest setting of UV-light keeping constant the concentration of H_2O_2 (Figure 2). The initial trial experiments were performed at different pH values from 2 to 4 with an arbitrarily selected value of UV and H_2O_2 concentration but with prior experience. After that, the dose of H_2O_2 and intensity of UV light were tuned at the pH obtained in the trial run. Further, pH was varied 2–4 with the best setting of UV and H_2O_2 concentration obtained before. We have checked at alkaline regions (pH = 11 and 13) for the CHPL removal but didn't get any significant results. Auspiciously, both the experiments at changing pH show the same pH value (Figure 2). Keeping the other two constant parameters, with increasing one of them, CHPL decomposition reached a maximum and then decreased and was ultimately stable at constant removal efficiency. The maximum removal

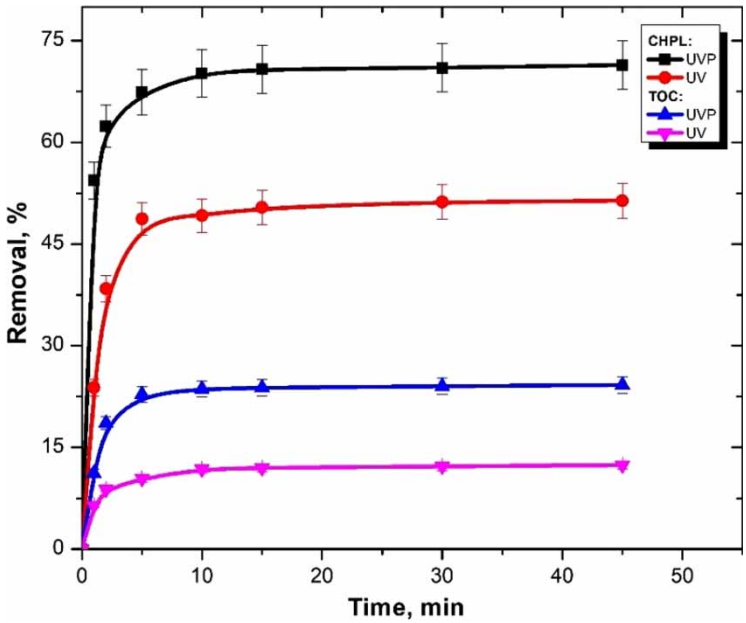

Figure 2 | CHPL and TOC removal with reaction time in photolytic reaction with a UV lamp of 9 W. Experiment conducted at $[CHPL]_0 =$ 100 mg/L with pH 3.0, $H_2O_2 = 15$ mM and temperature = 25 °C.

of CHPL obtained in UVP under an optimal condition was 71.4% with UV-irradiation. UVP gave significantly higher CHPL and TOC reductions compared to UV alone (Figure 2). Figure 2 showed that CHPL and TOC removal were found in two discrete rate periods. The transition was sharp and dramatically changed from 2.5 to 10 min for both CHPL and TOC reduction. At 2.5 min, the removal of CHPL was found to be 62.7% and increased to 71.2% in 10 min in the case of UVP. Whereas UV alone shows the shifting from 17.4% to 21.3% in time from 2.5 to 10 min for the same. In the presence of UV light alone the functional groups (=CO, –OH, –NHCOR) presence inside the amide chain of CHPL could disappear (Sykes 1985).

UPV and UV showed the TOC reduction of about 37–48% and 9–11% at 2.5 and 10 min of oxidation in UVP and UV, respectively. Initially, the mineralization of the amide chain in CHPL showed the faster rate of TOC removal. Tan *et al.* (2017) suggested that the maximum TOC removal of 31.7% was observed in 120 min at an initial concentration of 0.03 mM of CHPL. The second stage, probably after 10 min, was associated with the cleavage of $–NO_2$ functional group in substituted phenyl ring of CHPL molecule followed by mineralization. Kavitha & Palanivelu (2004) reported that intermediates were usually either fragmented or mineralized to lower molecular weight daughter molecules like oxalic and acetic acid that are mineralized rapidly in the presence of UV-illumination during the initial stage of oxidation.

Mean oxidation number of carbons

In this section, the concept of the mean oxidation number of carbon (MONC) is presented. We can obtain significant information by combining TOC and COD measurements when oxidative transformations of organic carbon are involved. MONC gave an idea of the experimental errors incurred in COD and TOC measurements. Chemically, the MONC must vary in the range between −4 for CH_4 to +4 of CO_2 (Zhao *et al.* 2010). The MONC for a single organic molecule with 'n' a number of carbon atoms can be represented as in Equation (3). Where, ON_i indicates the oxidation number of i^{th} carbon atom and the oxidation number of the individual carbon atom in round parenthesis for the CHPL molecule shown in Figure 1. For the C-C σ- and π-bonds; C = C σ- and π-bonds; and C = O σ- and π-bonds the corresponding oxidation numbers were 0, +1, +0.5 and +2, respectively (Park *et al.* 2002).

$$\text{MONC} = \frac{\sum_{i=1}^{n} \text{ON}_i}{n} \tag{3}$$

COD and TOC values are expressed in mg/L also could be combined to calculate the MONC irrespective to the number of organic fragments present in the sample (Equation (4)) (Dong *et al.* 2017).

$$\text{MONC} = 4 - 1.5\frac{\text{COD}}{\text{TOC}} \tag{4}$$

The COD value was experimentally determined and employed for the determination of MONC. The results are explored in Figure 3. MONC values initially estimated using either of two Equations (3) and (4) were found as 0.367. It indicates that both TOC and COD were determined with rational precision. The MONC was increased faster until <5 min, and then it improved progressively. The MONC elevated to 1.98 and 0.89 from 0.367 as initial value in 45 min of UVP and UV alone, respectively. The result can be verified by the refractory nature of the phenyl ring.

Role of foreign anions

Effects of selected inorganic anions were investigated on UV/H_2O_2 mediated degradation of CHPL (Figure 4). Few inorganic ions such as F^-, Cl^-, NH_4^+, HCO_3^- and NO_3^- were found to be played significant role during the remediation of CHPL (Li *et al.* 2020). In this study, some inorganic anions like NO_3^-, Cl^- and HCO_3^- were added individually, and their effects on CHPL degradation was explored. The concentration of each anion was 10 mM, and the results are plotted in Figure 4. The addition of ions influenced the degradation of CHPL in the order of $Cl^- > NO_3^- > HCO_3^-$. The fast reactivity of Cl^- with $HO^\cdot$ as shown in reaction (Equation (5)), possibly greatly seized the reactivity of $HO^\cdot$ with CHPL and consequently caused more inhibition in CHPL degradation. Li *et al.* reported a similar statement about the reactivity of Cl^- with $HO^\cdot$ for the degradation of ciprofloxacin drug (Li *et al.* 2020).

CHPL removal was about 71.2% without adding foreign anions in UVP. It decreased to 63.8, 65.4, and 67.2% at 45 min in the presence of Cl^-, NO_3^- and HCO_3^-, respectively (Figure 6). Homolytic C-Cl bond-breaking could occur in presence of UV-light. Cl^-, NO_3^- and HCO_3^- revealed a net reduction in CHPL degradation of 7.4, 5.8, and 4.9%, respectively in UVP compared to in UPV in absence of anions. Although, CHPL degradation was not affected significantly in the presence of HCO_3^- anion. The above results evidence that inhibition efficiency of Cl^- ion will be more than NO_3^- and HCO_3^- yielded

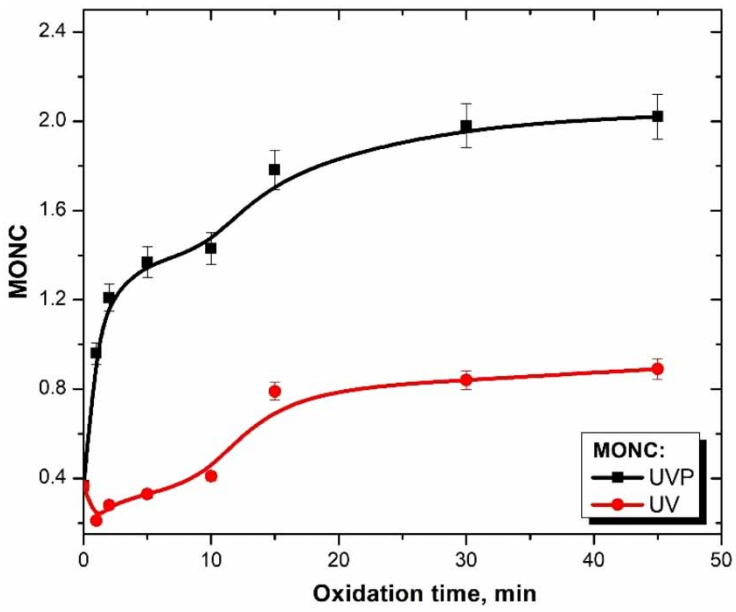

Figure 3 | Variation of MONC in UVP and UV: Experimental conditions: $[CHPL]_0 = 100$ mg/L, pH = 3.0, $H_2O_2 = 15$ mM and temperature = 25 °C.

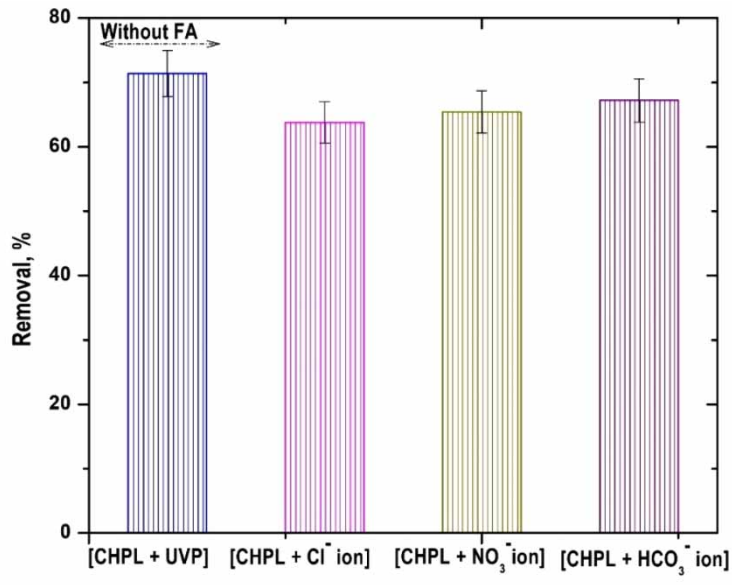

Figure 4 | Effect of foreign ions on CHPL removal in UVP. Experimental condition: $[CHPL]_0 = 100$ mg/L, pH = 3.0, $H_2O_2 = 15$ mM, $[Cl^-] = [F^-] = [NO_3^-] = 10$ mM, reaction time = 45 min, UV lamp = 9 W and temperature = 25 °C.

upon CHPL degradation (Figure 4).

$$Cl^- + HO^\bullet \leftrightarrows ClHO^{\bullet -}; \quad k = 4.3 \times 10^9\ M^{-1}s^{-1} \tag{5}$$

$$Cl^- + Cl^\bullet \leftrightarrows Cl_2.^-; \quad k = 6.5 \times 10^9\ M^{-1}s^{-1} \tag{6}$$

$$OH^- + Cl^\bullet \leftrightarrows ClOH^{\bullet -}; \quad k = 1,8 \times 10^{10}\ M^{-1}s^{-1} \tag{7}$$

Reaction between Cl^- and $HO^\cdot$ forming $ClHO^{\cdot -}$ (Equations (5)–(7)) is reversible that leads to increase of Cl^- concentration and inhibits the decomposition of CHPL by $HO^\cdot$ consumption (Deng *et al.* 2019).

$$NO_3^- + h\nu \rightarrow NO_2^- + 1/2O \tag{8}$$

$$NO_2^- + HO^\bullet \rightarrow NO_2^\bullet + OH^- \tag{9}$$

$$HCO_3^- + HO^\bullet \rightarrow H_2O + CO_3^{\bullet -}; \quad k = 3.9 \times 10^8\ M^{-1}s^{-1} \tag{10}$$

$$CO_3^{2-} + HO^\bullet \rightarrow OH^- + CO_3^{\bullet -}; \quad k = 8.5 \times 10^6\ M^{-1}s^{-1} \tag{11}$$

Deng *et al.* showed that NO_3^- could hinder the removal efficiency of the micropollutants. NO_3^- is strongly sensitive towards UV and acts as $HO^\cdot$ scavenger (H_2O_2) (Equation (8)). But the influence of NO_3^- was probably through NO_2^- for the drug degradation in the present study (Equations (10) and (11)). NO_3^- ions also show an important role in UVP due to conversion to nitrite (NO_2^-) (Csay *et al.* 2012). The production of $HO^\cdot$ radicals were also hindered because of NO_3^- photolysis (Equations (8) and (9)). Park *et al.* suggested that the remediation of volatile organic carbon (VOC) occurred by the inhibiting effect of NO_2^- during photolysis and $HO^\cdot$ radical depletion occurred due to progressive accumulation of NO_2^- (Csay *et al.* 2012).

Proposed mechanistic routes for CHPL degradation

The intermediate reaction products originated during UVP process of CHPL were analyzed by the HPLC-MS/MS, LC-QTOFMS, and IC analysis with ESI^+ mode. The chromatogram for the degradation products is available in the Supplementary Information (Fig. S4). The proposed mechanism is illustrated under the optimal time of 45 min reaction time. There are four mechanistic pathways (paths 1–4) of CHPL oxidation were proposed in Figure 5(a) and 5(b). Thirteen daughter intermediates were found in this study (Figure 4), and their detailed information is given in Table S1. Two asymmetry centers (C_1 and C_2) in

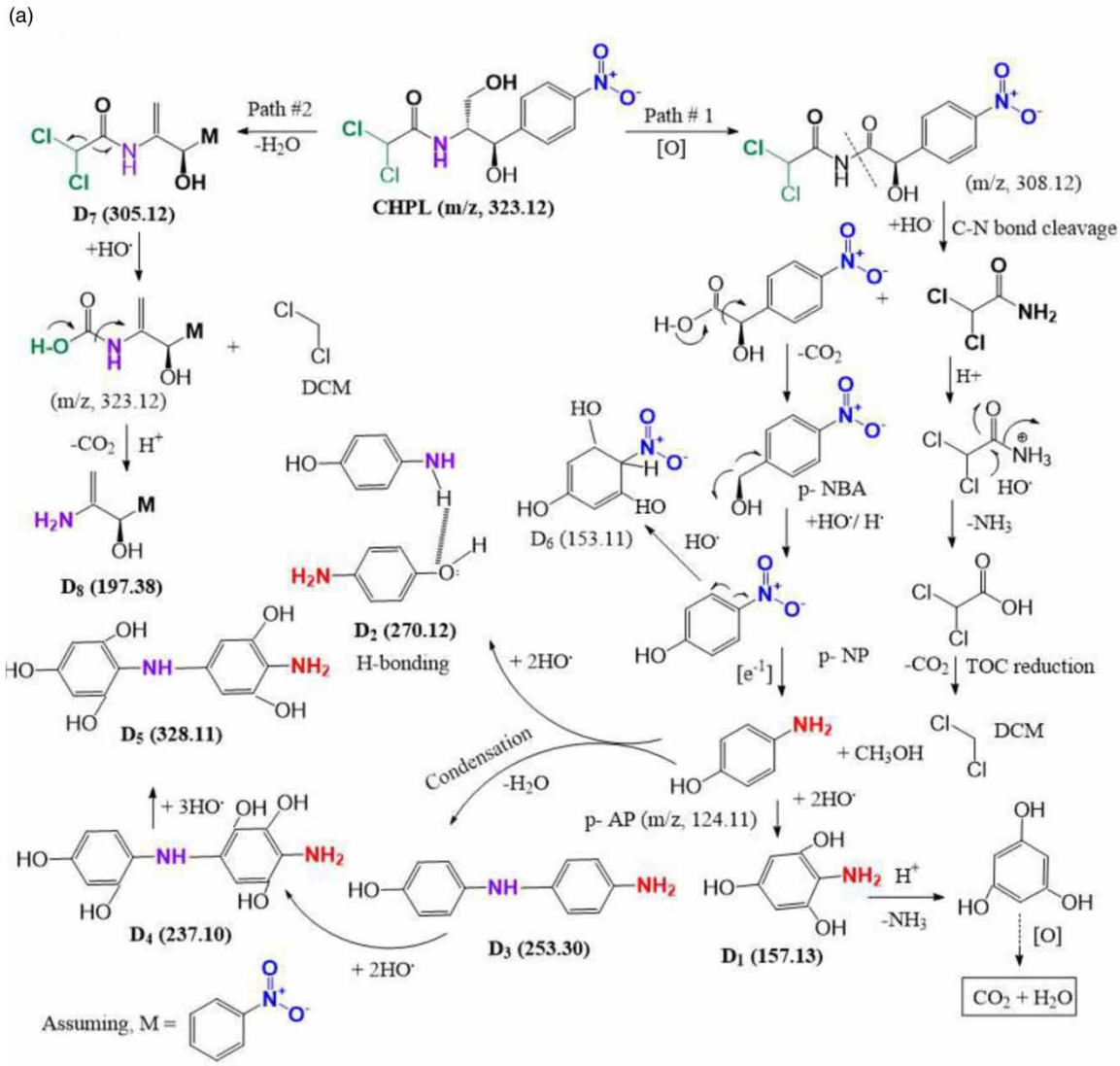

Figure 5 | (a) Proposed mechanistic pathways for CHPL degradation with the mass to charge (m/z) ratio in UVP. (b) CHPL degradation pathways. Continuation of cleavage of D_8 cleavage. (*Continued*).

CHPL with hydrogen atoms that were weakly bonded to each other. HO˙ radical could easily abstract these protons from these centers (Puma & Yue 1991). The presence of the amide group (-CONHR) attached to the C_2 center increased the nucleophilicity of both center (Puma & Yue 1991). Giri *et al.* stated that the carbonyl carbon (=CO) becomes more nucleophilic in character due to two chlorine (–Cl) atoms in the amide side chain at their geminal position (Levard *et al.* 2013).

Therefore, the shifting tendency of a lone electron in chlorine atom towards the carbonyl carbon is there. D_3 with m/z 171.13 was yielded for the attack of HO˙ radical at C_1 asymmetric center. Therefore, the C_1-C_2 bond in the side chain of the CHPL molecule is broken easily under the attack of HO˙ radicals, and then the substituted amino ($–NH_2$) group is easily oxidized to form p-nitro benzyl alcohol because of the lower C-N bond energy (Nie *et al.* 2014). Many hydroxylated products were yielded after CHPL degradation because of the addition of hydroxyl (–OH) or carbonyl (=CO) group on the CHPL structure (Aresta *et al.* 2010).

Thirteen fragments (D_1–D_{13}) were found in mass spectra in 45 min of UPV. From the difference between the proposed and exact masses of daughter ions, mass errors were calculated. Generally, low mass errors were gained from the fragmented molecules (Table S1). Four paths showed the formation of D_1, D_2, D_3, D_4, D_5, D_6, D_7, D_8, D_9, D_{10}, D_{11}, D_{12}, and D_{13} with molar masses of 157.13, 270.12, 253.30, 237.10, 328.11, 153.11, 305.12, 197.38, 167.21, 242.3, 214.09, 198.21, 340.11 and 283.10,

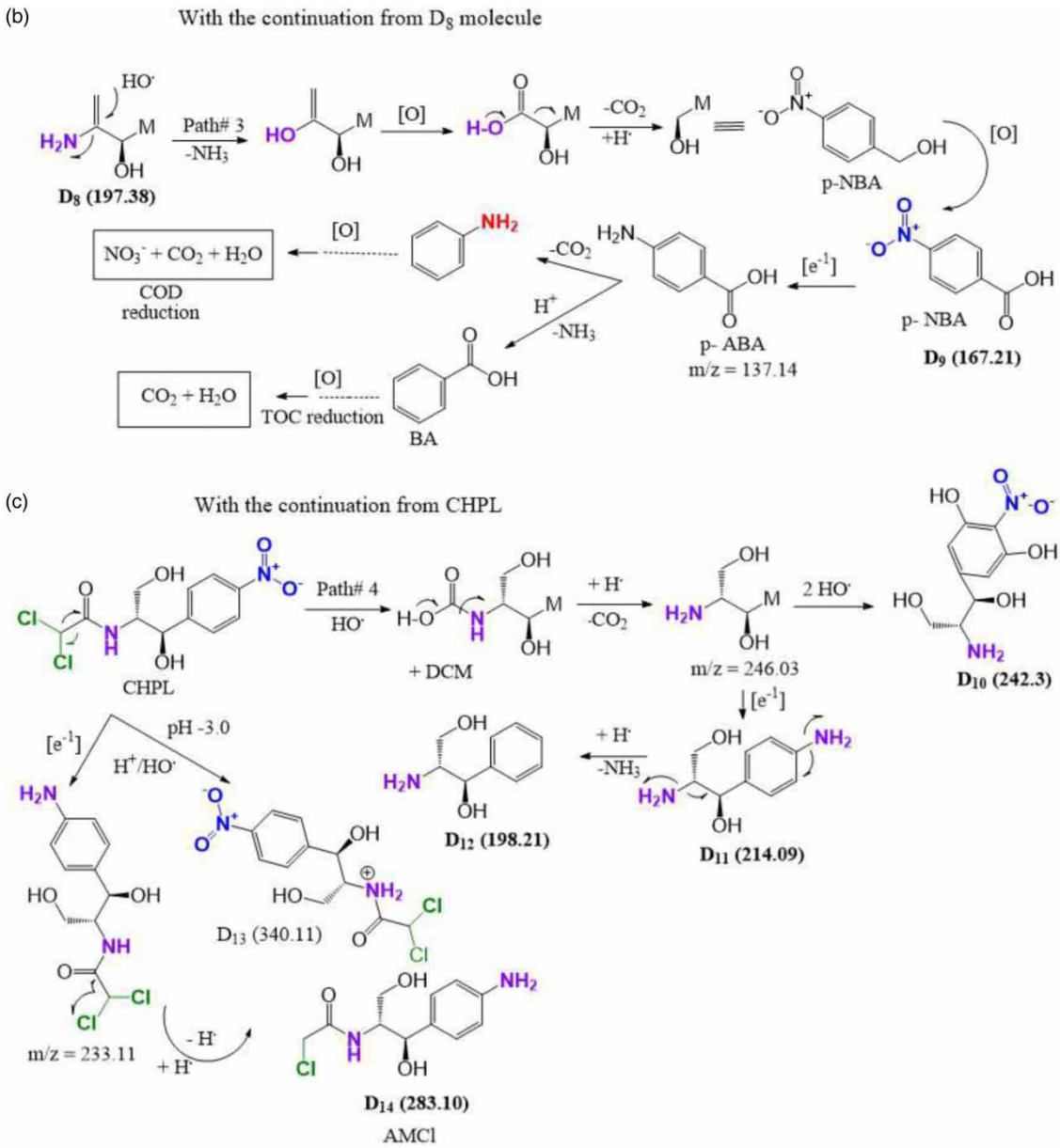

Figure 5 | Continued.

respectively (Figure 5(a) and 5(b)). The molar masses were expressed in terms of mass to charge (m/z) ratio. CHPL molecule is first oxidized at C_2 center to form an intermediate of molar mass 308.12, which produced dichloroacetamide and p-nitrobenzyl alcohol under C-N bond cleavage and hydrolysis followed by decarboxylation ($-CO_2$), respectively. Dichloroacetamide gets hydrolyzed at pH 3.0 and was converted to dichloromethane (DCM) with the evaluation of NH_3 and CO_2 that leads to evidence for the reduction of both COD and TOC (Figure 5(a)). P-amino phenol (p-AP) (m/z, 124.11) is the reduced product originated from p-nitrobenzyl alcohol through the reduction of p-nitrophenol and evidencing of the reduction of toxicity. Path #1 shows the formation path of D_1 to D_6 with m/z of 157.13, 270.12, 253.30, 237.10, 328.11 and 153.11, respectively. D_1 was yielded in UVP with low mass error (0.06 g/mol) through the amide chain cleavage followed by hydroxylation of CHPL molecule shown in path #1 (Figure 5(a)). D_2 and D_3 are produced from the p-AP through hydroxylation and dehydration reactions, respectively (Figure 5(a)). Hence, D_2 was originated from p-aminophenol (p-AP) with the molar mass of 124.11 by an intermolecular hydrogen bonding between them and was yielded by the reduction of $-NO_2$ group

at p-position. An intermolecular H-bonding between p-AP molecules appeared from the partial charge ($\delta^+ \ldots \delta^-$) separation on oxygen and hydrogen atoms in –OH and –NH_2 groups (Du *et al.* 2006). D_2 dimer molecule was identified in UVP. UV irradiation could easily break such weak H-bond (Sykes 1985). Again, D_4 and D_5 were hydroxylated products originated from D_3 molecule through hydroxylation reaction. Hence, an electrophilic substitution reaction was occurred effectively into D_3 due to the +R effect of the -NH_2 group that increases electron clouds in the phenyl ring (Tan *et al.* 2013). In the presence of UV light, the stability of CHPL could lose due to the high capability of light absorption within its functional groups that depends on electron distribution. The order of light absorption capacity of sigma (σ) bonds are very little above 200 nm and falls in the order of C-H > C-C > C-O > O-H), whereas pi (π) bonds (–COOH, = CO) and the ability of the compounds especially in conjugated pi systems are increased to absorb UV light at 254 nm by lowering the net energy difference between ground and excited states (Feiven *et al.* 2002). Double bond equivalent (DBE) indicates the degree of unsaturation of an organic molecule (Table S1) and signifies the number of molecules of H_2 that would have to be added to a molecule to convert all π-bonds to σ- bond. It was calculated by the summations of the residual ring(s) and the total number of pi bonds (π) (Kavitha & Palanivelu 2004). UVP showed hydroxylated compounds showed higher DBE (Figure 5(a) and 5(b)).

The formation of D_7 and D_8 molecules was shown in path #2. D_7 was yielded due to dehydration of CHPL, and D_8 was originated by hydroxylation followed by decarboxylation (-CO_2) of D_7 molecule along with the formation of DCM. Hence, decarboxylation of the –COOH group of the intermediate with molar mass 251.4 originated D_7 fragment was significantly happened because of the presence of an electron-withdrawing –NO_2 group. D_7 molecule is broken down to form D_9 shown in path #3 with the evaluation of ammonia (NH_3) and CO_2. D_9 (p-nitrobenzoic acid) undergoes further reduction to form p-aminobenzoic acid (p-ABA) and ultimately transferred to CO_2, NO_3^- and H_2O, that confirms for an effective COD reduction. In addition, D_{10} to D_{14} products were formed through path #4, where CHPL gets cleavage in different routes apart from paths #1, 2, and 3 (Figure 5(b)). D_{10} originated from CHPL with a series of successive reactions associated with the decarboxylation (–CO_2) reaction followed by hydroxylation along with the formation of DCM. Hence, DCM is originated as the CHPL containing a group (–$CHCl_2$) that could be decomposed to DCM and chlorine-free radical ($Cl^{\cdot}$) under the UV-light (Zhang *et al.* 2009). D_{11} molecule was yielded from the intermediate with m/z of 246.03 due to the reduction of –NO_2 group (Figure 5(b)). Under an acidic condition (pH 3.0), –NH_2 group in D_{11} is protonated and goes to form D_{12} with the liberation of NH_3. D_{13} is a direct hydrolyzed product of the CHPL molecule. D_{14} (AMCl) was originated from CHPL under reduction followed by dehydrohalogenation (–HCl) reaction (Figure 5(b)). Hence, –NO_2 group is reduced to –HN_2 group and Cl atom is removed through homolytic bond cleavage that gives evidence for the antimicrobial activity reduction. Zhang *et al.* (2009) suggested that D_{14} (AMCl) is less toxic in nature towards microorganisms and could be easy biodegradable. The reduction of CHPL to D_{14} would have environmental significance in terms of antibiotic elimination for the generation of antibiotic-resistant bacteria/genes in the environments (Nie *et al.* 2018). This observation strongly recommended that the final D_{14} has much less antibacterial activity than CHPL.

Kinetics for CHPL degradation

CHPL molecules are oxidized by $HO^{\bullet}$ radicals instantly and act as common oxidants (Equation (12)), and the fragmented products are formed. The reaction temperature of the solution was measured in a small range (23–25 °C). The pH difference was not shown significantly during the degradation of the drug. It was supposed that only active $HO^{\bullet}$ radical among the other reactive oxidation species (ROS) is involved to cleavage the CHPL drug in the solution.

$HO^{\bullet}$ radical was employed for CHPL oxidation (Equation (13)), and the initial CHPL concentration was fairly high compared to $HO^{\bullet}$ (results are shown here). The degradation of CHPL in UVP followed pseudo-first-order kinetics ($R^2 > 0.97$) as $HO^{\bullet}$ radical is a very nonselective and short-lived species (Figure 6(a) and 6(b)). Therefore, the rate equation is expressed in terms of concentration of CHPL only (Equation (14)). Where k_{obs} is the pseudo-first-order rate constants expressed in min^{-1}. CHPL and $HO^{\bullet}$ in square digression showed their concentration.

$$\text{CHPL} + \text{HO}^{\bullet} \rightarrow \text{Oxidized products} \tag{12}$$

$$-\frac{d[\text{CHPL}]}{dt} = k_1\,[\text{CHPL}][\text{HO}^{\bullet}] \tag{13}$$

$$-\frac{d[\text{CHPL}]}{dt} = k_{obs}\,[\text{CHPL}] \tag{14}$$

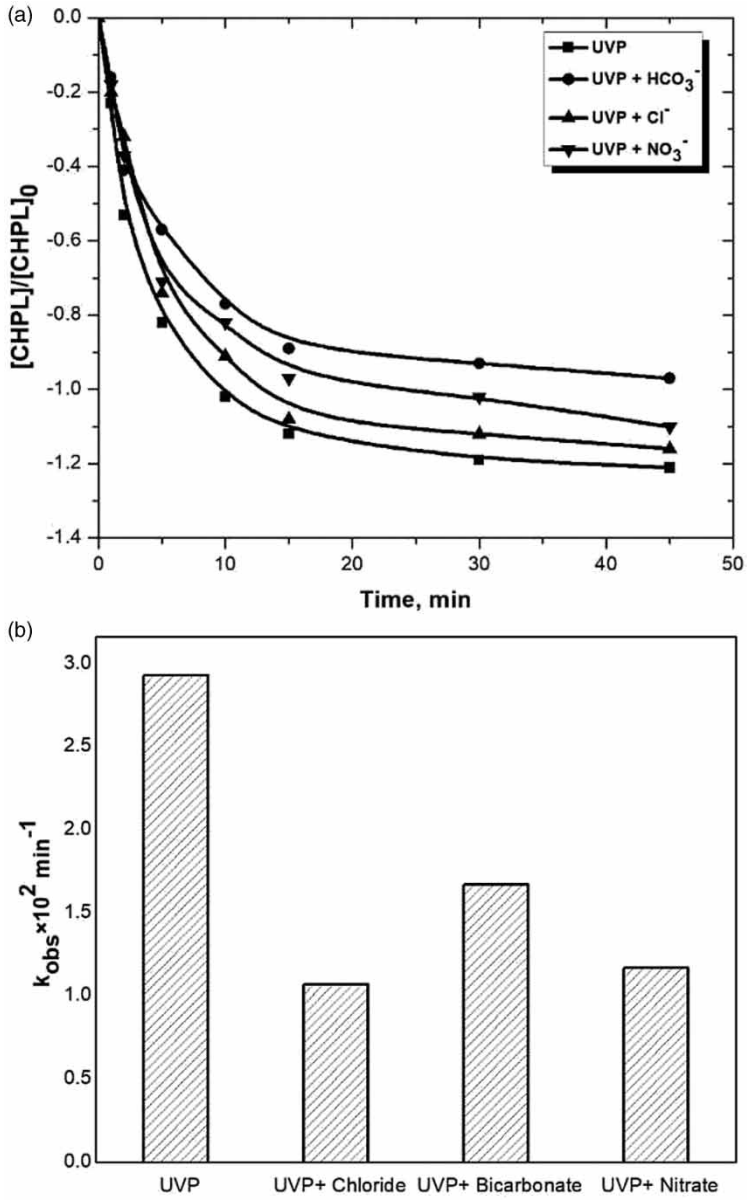

Figure 6 | (a) Variation of CHPL concentration profile in presence of foreign ions. Experimental condition: $[CHPL]_0 = 100$ mg/L, pH = 3.0, $H_2O_2 =$ 15 mM, $[Cl^-] = [F^-] = [NO_3^-] = 10$ mM, reaction time = 45 min, UV lamp = 9 W and temperature = 25 °C. (b) Effect of anions on CHPL degradation fitted with pseudo-first-order kinetics in UVP. Experimental condition: $[CHPL]_0 = 100$ mg/L, pH = 3.0, $H_2O_2 = 15$ mM, $[Cl^-] = [F^-] = [NO_3^-] =$ 10 mM, reaction time = 45 min, UV lamp = 9 W and temperature = 25 °C.

The overall rate equation for the reaction between CHPL and $HO^{\cdot}$ radical can be expressed using Equation (15).

$$\ln \frac{[CHPL]}{[CHPL]0} = -k_{obs} \times t \tag{15}$$

where, $[CHPL]_0$ and [CHPL] represents the molar concentration of CHPL at time 0 to t, respectively. The kinetic constant for CHPL oxidation was determined by the least square technique. The graphics are best fitted shown in Figure 6(a) and 6(b). The results suggested that CHPL degradation followed the pseudo-first-order kinetics. In UVP, the fitted k_{obs} was found as $2.93 \times 10^{-2}\,min^{-1}$. As shown in Figure 6(b), the CHPL degradation rate constant continuously decreased in presence of foreign anions like Cl^-, NO_3^- and HCO_3^- and followed pseudo-first-order kinetics. It was found that Cl^- exhibited more inhibition

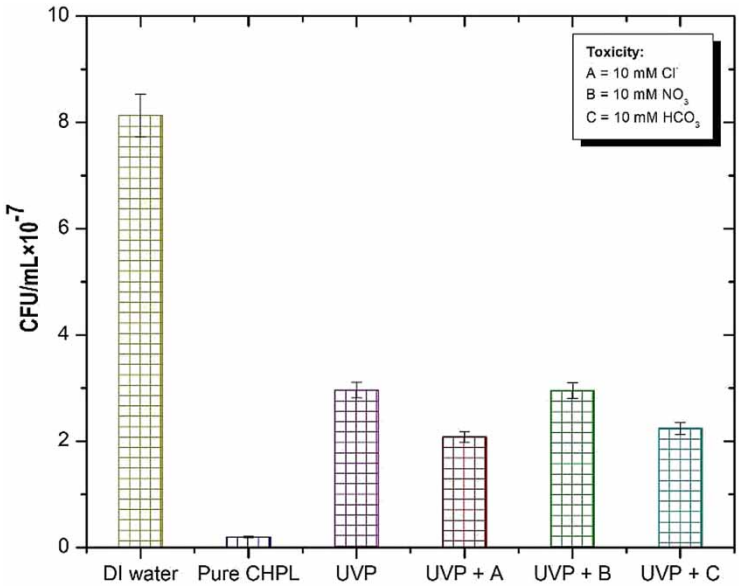

Figure 7 | Growth of *E. coli* strain after 24 h of exposure to CHPL along with intermediate mixture after 45 min during UPV. Experimental condition: $[CHPL]_0 = 100$ mg/L, pH = 3.0, $H_2O_2 = 15$ mM, $[Cl^-] = [F^-] = [NO_3^-] = 10$ mM, reaction time = 45 min, UV lamp = 9 W and temperature = 25 °C.

effects on the CHPL degradation efficiencies than other anions with the same molar concentrations of 10 mM. In addition, the curve was well fitted, and the k_{obs} were 1.07×10^{-2} min^{-1} (Figure 6(b)). A pseudo-first-order kinetics for the oxidation of CHPL with the rate constant in the presence of persulphate oxidation was found 1.18×10^{-2} min^{-1} in the presence of Cl^- with the molar concentration of 100 mM (Csay *et al.* 2012). It is believed that Cl^- is a strong reactive species to scavenge HO· radicals will further promote the degradation of CHPL in the system (Zuorro *et al.* 2014).

NO_3^- has also strong inhibition effects on CHPL removal, and this effect is increased with increasing NO_3^- concentrations. In the presence of NO_3^-, the rate constant (k_{obs}) suddenly decreased from 2.93×10^{-2} min^{-1} to 1.17×10^{-2} min^{-1} in UVP. Tan *et al.* reported a close value of the rate constant of 0.97×10^{-2} min^{-1} on the degradation of chloramphenicol in water by UV/persulfate system (Nie *et al.* 2018). The similar effect of HCO_3^- on the CHPL degradation was found, and the rate constant dropped to 1.67×10^{-2} min^{-1} in UVP. Li *et al.* showed that the pseudo-first-order rate constant was found as 1.55×10^{-2} min^{-1} in the presence of HCO_3^- on the chloramphenicol degradation during nZVI-heat-activated persulphate oxidation.

Antimicrobial activity of CHPL and its degradation products

The effectiveness of the UVP process was assessed in terms of antibiotic activity removal against *E. coli* pathogens. The toxicity of CHPL and its decomposition products in UPV to *E. coli* in LB media (10 g peptone +5 g yeast extract +5 g NaCl +10 g agar) after 24 h of exposure was shown in Figure 7. Pathogen *E. coli*, as the gram-negative bacteria is highly sensitives towards CHPL (Nie *et al.* 2018). The activity of *E. coli* was measured in the CHPL solution in UVP treatment under optimal conditions.

The growth of *E. coli* was almost inhibited in the presence of 100 mg/L of CHPL entirely was found to be 0.23×10^7 CFU/mL (Figure 7). In toxicity analysis, the growth of *E. coli* was found 8×10^7 CFU/mL in the presence of LB media and deionized water. The growth of *E. coli* strain was inhibited after 24 h of exposure in the presence of 32 mg/L CHPL (Liang *et al.* 2013).

The toxicity in UVP and UVP in presence inorganic ions were comparable. The exposure of toxicity to *E. coli* was more in UVP in the presence of Cl^- even though there was no significant difference between Cl^- and NO_3^- in UVP as the HO· radicals scavenging ability of both ions the same. The addition of ions influenced the order of toxicity of CHPL degraded products as $Cl^- > NO_3^- > HCO_3^-$ (Figure 7). About 62.8, 49.7, 47.7, and 53.7% cell death were noticed after 24 h contact of *E. coli* in the reaction mixture collected after 45 min of UVP, UVP in the presence of Cl^-, NO_3^- and HCO_3^-, respectively, in comparison to the control condition (Figure 7). It has been found that the product D_{14}, hydroxylamine chloride intermediate (AMCl) lost its antimicrobial activity significantly than pure CHPL due to the reduction of $-NO_2$ group and the elimination of $-Cl$· radical in terms of HCl (Figure 5(b)). Liang *et al.* showed similar observations for the same intermediate AMCl when CHPL is reduced with biocathode of applied voltage of 0.5 V in a bioelectrochemical system (Liang *et al.* 2013). Two amine products obtained

under CHPL cleavage (D_{11}) and a novel dechlorinated product (D_{14}) were identified in this study (Figure 5(b)) and also showed evidence for the reduction of toxicity. P-nitrophenol and p-nitro benzyl alcohol intermediates are toxic in nature, and the firster one was identified in UVP. Both molecules were mineralized into CO_2, NO_3^- and H_2O (Finar 2001; Demir *et al.* 2010).

CONCLUSIONS

The degradation of CHPL was investigated by UV/H_2O_2 photolysis advanced oxidation process. The following conclusions are explored in our study:

1. The maximum CHPL and TOC removal of 72.4% and 51.3%, respectively, were found with initial CHPL concentration of 100 mg/L at optimum conditions.
2. CHPL removal were 21.3% and 71.2% at 45 min when treated in UV alone and UVP, respectively. It dropped to 63.8%, 65.4% and 67.2% in the presence of Cl^-, NO_3^- and HCO_3^-, respectively.
3. UVP exhibited TOC removal of 47.8% and 11.0% in UVP and UV alone, respectively.
4. The MONC was found to be increased from 0.367 to 2.02 in UVP at the optimal conditions.
5. Measurement of toxicity and the MONC have given the information about the production of low toxic compounds and an idea of the experimental errors between COD and TOC analysis.
6. Thirteen fragmentations with m/z ratio were primarily formed upon CHPL degradation in UVP. Hydroxylation and decarboxylation reactions were significantly found for the CHPL cleavage.
7. A pseudo-first-order kinetic model for the cleavage of CHPL in UVP exhibited good fittings to the experimental data. Rate constant for CHPL degradation was found to be 2.93×10^{-2} min^{-1} where as in presence of Cl^-, NO_3^- and HCO_3^- ions, k_{obs} were found as 1.07×10^{-2} min^{-1}, 1.17×10^{-2} min^{-1} and 1.67×10^{-2} min^{-1}, respectively.
8. The toxicity of intermediates was found to be increased in presence of foreign ions. D_{11} and D_{14} products showed decrease in antimicrobial activity due to reduction of $-NO_2$ group which is present in these molecules.

DATA AVAILABILITY STATEMENT

All relevant data are included in the paper or its Supplementary Information.

REFERENCES

Aouiche, A., Sabaou, N., Meklat, A., Zitouni, A., Bijani, C., Mathieu, F. & Lebrihi, A. 2012 Saccharothrix sp. PAL54, a new chloramphenicol-producing strain isolated from a Saharan soil. *J. Microbiol. Biotechnol.* **28**, 943–951.

APHA 1998 *Standard Methods for the Examination of Water and Wastewater*, 20th edn. American Public Health Association, Washington, DC, USA.

Aresta, A., Bianchi, D., Calvano, C. D. & Zambonin, C. G. 2010 Solid phase microextraction-Liquid chromatography (SPME-LC) determination of chloramphenicol in urine and environmental water samples. *J. Pharm. Biomed. Anal.* **53**, 440–444.

Boxall, A. B. A., Fogg, L. A., Kay, P., Blackwell, P. A., Pemberton, E. J. & Croxford, A. 2003 Prioritisation of veterinary medicines in the UK environment. *Toxicol. Lett.* **142**, 207–218.

Brooks, M. H., Smith, R. L. & Macalady, D. L. 1992 Inhibition of existing denitrification enzyme activity by chloramphenicol. *Appl. Environ. Microbiol.* **58**, 1746–1753.

Csay, T., Racz, G., Takacs, E. & Wojnarovits, L. 2012 Radiation induced degradation of pharmaceutical residues in water: Chloramphenicol. *Radiat. Phys. Chem.* **81**, 1489–1494.

Demir, E., Kocaoglu, S. & Kaya, B. 2010 Assessment of genotoxic effects of benzyl derivatives by the comet assay. *Food Chem. Toxicol.* **48**, 1239–1242.

Deng, J., Xu, M. Y., Chen, Y. J., Li, J., Qiu, C. G., Li, X. Y. & Zhou, S. Q. 2019 Highly-efficient removal of norfloxacin with nanoscale zero-valent copper activated persulfate at mild temperature. *Chem. Eng. J.* **366**, 491–503.

Dong, H., Qiang, Z., Hu, J. & Qu, J. 2017 Degradation of chloramphenicol by UV/chlorine treatment: kinetics, mechanism and enhanced formation of halo nitromethanes. *Water Res.* **121**, 178–185.

Du, Y. X., Zhou, M. H. & Lei, L. C. 2006 Role of the intermediates in the degradation of phenolic compounds by Fenton-like process. *J. Hazard. Mater.* **136** (3), 859–865.

Feiven, C., Pehkonen, S. O. & Ray, M. B. 2002 Kinetics and mechanisms of UV photodegradation of chlorinated organics inside the gas phase. *Water Res.* **36**, 4203–4214.

Finar, I. L. 2001 *Stereochemistry and the Chemistry of Natural Products*, 5th edn. Longman, London, UK.

Giri, A. S. & Golder, A. K. 2014 Formation of Fe(II)-Chloramphenicol chelate and its decomposition in Fenton and Photo-Fenton: identification and biodegradability assessment of primary by products. *Ind. Eng. Chem. Res.* **53** (42), 16196–16203.

Giri, A. S. & Golder, A. K. 2014 Ciprofloxacin degradation from aqueous solution by Fenton oxidation: reaction kinetics and degradation mechanisms. *RSC Adv.* **4**, 6738–6745.

Hu, X., Zhou, Q. & Luo, Y. 2010 Occurrence, and source analysis of typical veterinary antibiotics in manure, soil, vegetables and groundwater from organic vegetable bases, northern China. *Environ. Pollut.* **158**, 2992–2998.

Kavitha, V. & Palanivelu, K. 2004 The role of ferrous ion in Fenton and photo-Fenton processes for the degradation of phenol. *Chemosphere* **55**, 1235–1243.

Levard, C., Mitra, S., Yang, T., Jew, A. D., Badireddy, A. R., Gregory, V. & Brown, G. E. 2013 Effect of chloride on the dissolution rate of silver nanoparticles and toxicity to E. coli. *Environ. Sci. Technol.* **47**, 5738–5745.

Li, H., Yang, L., He, L., Ma, Y., Yan, X., Wu, L. & Zhang, Z. 2020 Kinetics and mechanisms of chloramphenicol degradation in aqueous solutions using heat-assisted nZVI activation of persulfate. *J. Mol. Liq.* **313**, 113511.

Liang, B., Cheng, H. Y., Kong, D. Y., Gao, S. H., Sun, F., Cui, D., Kong, F. Y., Zhou, A. J., Liu, W. Z., Ren, N. Q., Wu, W. M., Wang, A. J. & Lee, D. J. 2013 Accelerated reduction of chlorinated nitroaromatic antibiotic chloramphenicol by biocathode. *Environ. Sci. Technol.* **47**, 5353–5361.

Lin, A., Yu, T. & Lin, C. 2008 Pharmaceutical contamination in residential, industrial, and agricultural waste streams: risk to aqueous environments in Taiwan. *Chemosphere* **74** (1), 131–141.

Liu, H., Zhang, G., Liu, C. Q., Li, L. & Xiang, M. 2009 The occurrence of chloramphenicol and tetracyclines in municipal sewage and the Nanming River, Guiyang City, China. *J. Environ. Monit.* **11** (6), 1199–1205.

Luis, A. D., Lombranda, J. I., Varona, F. & Menendez, A. 2009 Kinetic study and hydrogen peroxide consumption of phenolic compounds oxidation by Fenton's reagent. *Korean J. Chem. Eng.* **26** (1), 48–57.

Miklos, D. B., Remy, C., Jekel, M., Linden, K. G., Drewes, J. E. & Hubner, U. 2018 Evaluation of advanced oxidation processes for water and wastewater treatment-A critical review. *Water Res.* **139**, 118–131.

MPEDA 2010 *Marine Products Export Development Authority Notification No. MAS/12/80-2002/QC dt. 20.05.2002.* Ministry of Commerce and Industry, Government of India, Chennai, India.

Nascimento, G. E., Oliveira, M. A. S., Santana, R. M. R., Ribeiro, B. G., Sales, D. C. S., Rodríguez-Díaz, J. M., Napoleão, D. C., Sobrinho, M. A. M. & Duarte, M. M. M. B. 2020 Investigation of paracetamol degradation using LED and UV-C photo-reactors. *Water Sci. Technol.* **81** (12), 2545–2558.

Nie, M., Yang, Y., Zhang, Z., Yan, C., Wang, X., Li, H. & Dong, W. 2014 Degradation of chloramphenicol by thermally activated persulfate in aqueous Solution. *Chem. Eng. J.* **246**, 373–382.

Nie, M., Yan, C., Xiong, X., Wen, X., Yang, X., lv, Z. & Dong, W. 2018 Degradation of chloramphenicol using a combination system of simulated solar light, Fe^{2+} and persulfate. *Chem. Eng. J.* **348**, 455.

Park, H., Kim, H. T. & Barak, K. 2002 The ferroxidase activity of yeast frataxin. *Eur. J. Med. Chem.* **37**, 443–448.

Parsley, L. C., Consuegra, E. J., Kakirde, K. S., Land, A. M., Harper, W. F. & Liles, M. R. 2010 Identification of diverse antimicrobial resistance determinants carried on bacterial, plasmid, or viral metagenomes from an activated sludge microbial assemblage. *Appl. Environ. Microbiol.* **76** (11), 3753–3757.

Puma, G. L. & Yue, P. L. 1991 Photocatalytic oxidation of chlorophenols in single component and multi-component systems. *Ind. Eng. Chem. Res.* **36**, 27–38.

Sa Da Rocha, O. R. 2013 Degradation of the antibiotic chloramphenicol using photolysis and advanced oxidation process with UVC and solar radiation. *Desal. Water Treat.*, 1–7. doi:10.1080/19443994.2013.792148.

Shen, Y. J., Xu, Q. H., Liang, J. & Xu, W. 2016 Degradation of Reactive YellowX-RG by O3/Fenton system: response surface approach, reaction mechanism, and degradation pathway. *Water Sci. Technol.* **74**, 2483–2495.

Sykes, P. 1985 *A Guidebook to Mechanism in Organic Chemistry*, 6th edn. Longman Scientific & Technical, New York, NY, USA.

Tan, C., Dafang, F., Gao, N.-Y., Qingdong, Q. & Yan, X. 2017 Kinetic degradation of chloramphenicol in water by UV/persulfate system. *J. Photochem. Photobiol. A.* **332**, 406–412.

Trovo, A. G., de Paiva, A. B. V., Machado, A. E. H., Carlos, A. & Santos, R. O. 2013 Degradation of the antibiotic chloramphenicol by photo-Fenton process at lab-scale and solar pilot plant: kinetic, toxicity and inactivation assessment. *Solar Energy* **97**, 596–604.

Wu, Y. T., Zhu, S. M., Zhang, W. Q., Bu, L. J. & Zhou, S. Q. 2019 Comparison of diatrizoate degradation by UV/chlorine and UV/chloramine processes: kinetic mechanisms and iodinated disinfection by products formation. *Chem. Eng. J.* **375**, 121–132.

Xiang, Y. Y., Fang, J. Y. & Shang, C. 2016 Kinetics and pathways of ibuprofen degradation by the UV/chlorine advanced oxidation process. *Water Res.* **90**, 301–308.

Zhang, X. X., Zhang, T. & Fang, H. H. P. 2009 Antibiotic resistance genes in water environment. *Appl. Microbiol. Biotechnol.* **82** (3), 397–414.

Zhang, T. & Li, B. 2011 Occurrence, transformation, and fate of antibiotics in municipal wastewater treatment plants. *Crit. Rev. Environ. Sci. Technol.* **41** (11), 951–998.

Zhao, Y., Huang, M., Tang, M. X. & Liu, L. 2010 The protein kinase Hal5p is the high-copy suppressor of lithium-sensitive mutations of genes involved in the sporulation and meiosis as well as the ergosterol biosynthesis in Saccharomyces cerevisiae. *Environ. Monit.* **21**, 271–279.

Zuorro, A., Fidaleo, M., Fidaleo, M. & Lavecchia, R. 2014 Degradation and antibiotic activity reduction of chloramphenicol in aqueous solution by UV/H_2O_2 process. *J. Environ. Manage.* **133**, 302–308.

First received 6 April 2021; accepted in revised form 17 June 2021. Available online 29 June 2021